REMOTE SENSING OF ATMOSPHERE AND UNDERLYING SURFACE USING RADIATION OF GLOBAL NAVIGATION SATELLITE SYSTEMS

Nguyen Xuan Anh[1,5*], Lutsenko V. I.[2], Popov D. O.[2], Cong Pham Chi[3], Trung Tran Hoai[4]

[1]*Institure of Geophysics, VAST, Vietnam*
[2]*Institute of Radiophysics and Electronics, Kharkov, Ukraine*
[3]*Vietnam Research Institute of Electronics, Informatics and Automation, Vietnam*
[4]*University of Communications and Transport, Vietnam*
[5]*Graduate University of Science and Technology, VAST, Vietnam*
[*]E-mail: nxuananh05@gmail.com

Received: 9-11-2017

ABSTRACT: This paper is devoted to solving the problem of atmosphere diagnosis using radiation of the global navigation satellites. New methods for diagnosing the meteorological situation, the refractive state of the troposphere and underlying surface based on the behavior of navigation signals are proposed. The model of the mapping function that takes into account the sphericity of the troposphere and allows more accurate describing of the actual values for the tropospheric delay is proposed.

Keywords: Radio wave propagation, tropospheric refraction, refractive index, daily and seasonal variability, global navigation satellite system, underlying surface.

INTRODUCTION

The study of physical processes in the troposphere is necessary to understand the unstable atmospheric manifestations that cause weather changes, as well as the factors that determine the statistical properties of the general circulation of the atmosphere. It is known that the effectiveness of the operation of radio systems for different purposes (navigation, radar, communication), mostly depends on the radio wave propagation conditions. Today, there is a significant electromagnetic "pollution" of the environment, and therefore it seems extremely attractive to use existing satellites (navigation, meteorology or television) for monitoring of the atmospheric processes and hazardous nature phenomena. In the report one discusses methods for remote sensing of atmospheric processes and the underlying surface using the received signals of radio emission from satellites of the global navigation systems GPS, GLONASS.

MAIN PART

The basic idea is to use the radio emission of existing satellites to create a system for global monitoring of atmospheric processes and hazardous meteorological phenomena. It is based on radio occultation method (the method of radio-eclipses), which has several varieties. The physical prerequisite of the method is the interrelation between the signal parameters and the measure of atmospheric refraction, as well as their dependence on the presence of dangerous meteorological phenomena on the propagation path.

Usually two-frequency precision measurements are used to diagnose the troposphere using GNSS, which makes possible to separate the influence of the ionosphere and the troposphere, and also to estimate the zenith delays for getting information about the moisture reserve of the troposphere [1-3]. From GPS data, it is possible to obtain measurements of Zenith Tropospheric Delay (ZTD), which consists of Zenith Wet Delay (ZWD) and Zenith Hydrostatic (Dry) Delay (ZHD):

$$ZTD = ZWD + ZHD \qquad (1)$$

ZHD can be easily calculated from terrestrial meteorological measurements using an empirical model that was developed for this purpose. The most popular models are Saastamonien (S), Hopfield (H) and Black (B), which look as follows [4]:

$$d_S^z = 0.2277 \cdot \frac{P}{F(\phi, H)} \qquad (2)$$

$$F(\phi, H) = 1 - 0.0026 \cdot \cos(2\phi) - 0.00028 \cdot H$$

$$d_H^z = \left(0.0023081 - 0.00758 \cdot \frac{1}{T_0}\right) \cdot P_0 \quad (3)$$

$$d_B^z = 0.2343 \cdot (T - 4.12) \cdot \frac{P}{T} \qquad (4)$$

Where φ is the latitude of the station in radian, H is the height of the station above sea level in kilometer, P is the surface air pressure in hPa, T is the absolute temperature in Kelvin.

The expressions show that all *ZHD* models require ground-based meteorological measurements, including air pressure and temperature, the accuracy of which will also affect the error in determining *ZWD*.

In the source [5], the following interrelation between the wet delay d_w and the total actual amount of precipitated water (PW_Φ):

$$Q = \frac{d_w}{PW_\Phi} = 10^{-8} \cdot \rho R_v \left[(k_3 / T_m) + k_2'\right] \quad (5)$$

Where ρ is the density of liquid water; R_v is the specific gas constant of water vapor, equal to 461.524 $J \cdot kg^{-1} \cdot K^{-1}$; k_2', k_3 are constants of atmospheric refraction; T_m is defined as follows.

$$T_m = \frac{\int \rho_v dz}{\int \frac{\rho_v}{T} dz} \qquad (6)$$

Where ρ_v is the density of water vapor; T is the temperature, z is the vertical coordinate.

In [3] it was noted that the drawback of existing models and methods for measuring the wet delay in the GPS/GLONASS navigation systems is that in assessing the wet delay, the part of the total amount of water and vapor rises to an absolute and does not take into account such a physical phenomenon as humidification of atmospheric aerosol. Meanwhile, the aerosol load of the atmosphere and the known degree of variability in the aerosol contamination of the troposphere lead to the fact that the actual dynamics of the total amount of water in the atmosphere depends not only on the movement of wet flows into the atmosphere, but also on the degree of atmospheric stagnation with fresh unmoistened aerosol [3]. According to the expression obtained in [3], the total wet delay is a function of not only the initial total value of the deposited water, but also the existing increment in the optical thickness of the atmospheric aerosol. According to [1], at a water vapor density of 25 g/m, the signal delay is 140 mm/km.

However, it is far from always possible to use high-precision two-frequency receivers and meteorological data, so it is advisable to develop approaches for more common single-frequency equipment. Since the single-frequency receivers don't have the ability to excrete tropospheric delay without additional instruments, the subject of analysis in the diagnosis of the surrounding space will be the increment of pseudorange. Under the pseudorange increment, we will understand the difference between the theoretical delay caused

by the geometric range from satellite to ground equipment and the real delay caused by the propagation path. It should be noted that the use of single-frequency receivers allows the detection of rain zones, but such meteorological phenomena, for example, fog or snow masks under daily fluctuations of the analyzed information, which makes it difficult to detect these phenomena. Tropospheric refraction and the presence of inhomogeneities in the troposphere, for example, in the form of clouds saturated with moisture, will lead to an increase in the pseudorange value to the navigation satellite and the appearance of errors in the coordinates measuring. The extension of the electric path of the electromagnetic wave, which propagates through the atmosphere, will be determined by the dielectric permittivity of the environment which depends on the moisture reserve.

In the case of rain, the geometric characteristics of its zones depend on the intensity and climatic conditions in the area of deposition [6]. It should be noted that the rains in their fall zone are unevenly distributed, especially the rains with an intensity of 40 mm/h and more. In [7] it is shown that the dependence of the attenuation coefficient on the rain intensity at its large values has an almost linear character. The change in pseudo-range Δr due to the passage of an electromagnetic wave through a zone with an increased moisture reserve W with a length Δl_0 will be $\Delta r = \delta r \Delta l_0$, and at small angles the extent of the zone will roughly correspond to its horizontal dimensions. Intensive rainstorms, thunderstorms, squalls and hail are associated with the multicellular class of cumulonimbus clouds, which are most often observed at mid-latitudes in summer (less often in spring and autumn). The diameter of the cluster of such clouds is about 10-15 km, and the thickness is 7-10 km.

Since the sensitivity to the presence of clouds increases at small elevation angles due to the increase in the path length in the sediments, the experiments for measuring of the pseudoranges to the satellites were made at their occultation over the horizon. On the basis of the theoretical calculations, it was shown (fig. 1), changes in pseudo-range can be expected with different characteristics of rain (intensity and size of their zone).
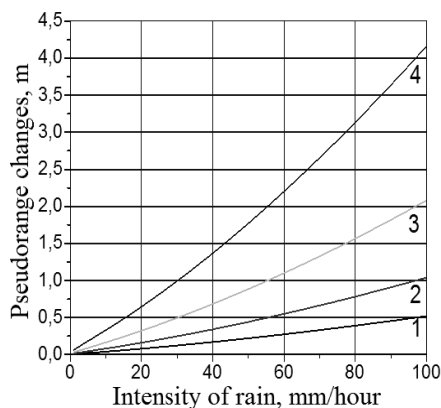

Fig. 1. Dependence of the growth of pseudorange on the intensity of precipitation and the size of their zone: 1) l_0=5 км, 2) l_0=10 км, 3) l_0=20 км, 4) l_0=40 км
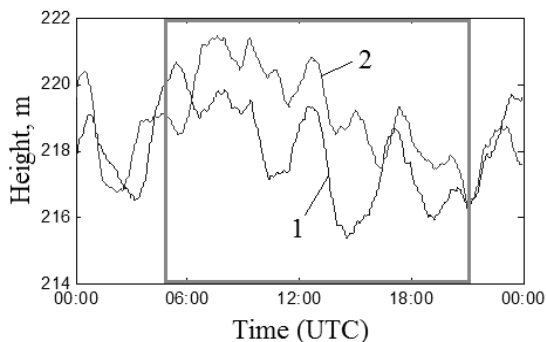

Fig. 2a. Changes in measured coordinate information: 1) during the rain, 2) stable meteorological conditions

In the standard session of navigational measurements, there are about 20 satellites of GPS and GLONASS systems, which ensure uniform covering of all azimuth directions. It should be noted that intensive rains will be localized and accordingly a change in pseudorange will be observed only in satellites whose trajectories pass through precipitation. Thus, a change in the pseudorange of a group of satellites in a certain azimuthal direction will lead to a shift in the measured coordinate

Nguyen Xuan Anh, Lutsenko V. I.,...

information in comparison with calm meteorological conditions (fig. 2a) [8]. Similar shifts of coordinate information during the passage of rain were obtained in the work [9] (fig. 2b), where changes in the coordinates of the fixed receiver were given depending on the weather conditions for 120 minutes.
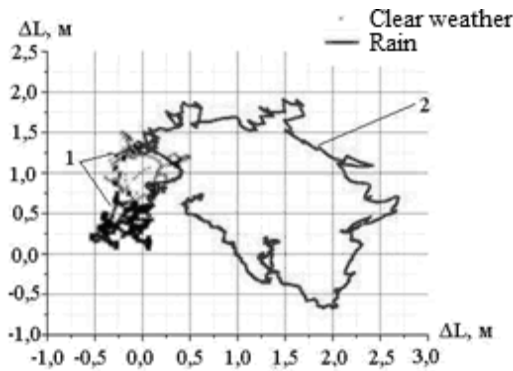

Fig. 2b. Change of coordinates under various meteorological conditions [9]: 1) stable solar, magnetic and meteorological conditions, 2) rain

The passage of rain essentially leads to a change in the refractive index of the troposphere. The conducted studies showed that the fluctuations of the plane coordinates with respect to the real position of the antenna are inversely related to the space-time variations of the refractive index around the measuring point. For the analysis, 10

meteorological stations were used, according to which the changes in the refractive index at 3 hour intervals (fig. 3c) and the data of the plane fluctuations of the measured coordinates of the stationary navigation receiver were estimated (fig. 3b).

In addition to detecting rain zones by estimating pseudorange variations, pseudorange increment values can be used at small viewing angles of satellites to determine the value of the gradient of the refractive index. Since a significant effect on the pseudorange increment due to refraction is observed at small viewing angles that are usually excluded from the navigation solution, it will be advisable to use this data in conjunction with the model of the tropospheric delay mapping function that takes into account the effect of refraction via the refractive index gradient. From the consideration of the model of a spherically layered troposphere, the mapping function was proposed [10]:

$$m_e(\beta) = \left(-1 + \sqrt{1 + \frac{1}{\sin^2 \beta}\left(\frac{2h_e}{a_e} + \frac{h_e^2}{a_e^2} \right)} \right) \frac{a_e}{h_e} \sin \beta$$

Where β is the elevation angle of satellite, h_e is the height of the troposphere, depends on latitude; a_e is the equivalent radius of the Earth.
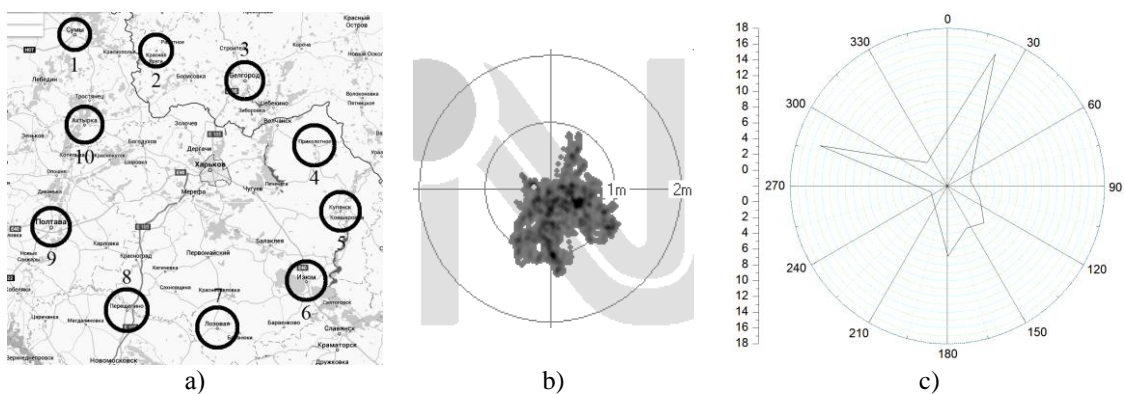

Fig 3. The location of meteorological stations for measuring of the refractive index (a), the planar coordinates (b) and the change in the refractive index (c) at 3-hour intervals

This mapping function, in contrast to existing ones, uses the equivalent Earth radius

model and takes into account the refractive properties of the troposphere. It should be

noted that the developed models of mapping functions that are used in coordinate correction sufficiently well take into account the errors associated with the influence of the propagation medium at operating angles (above 5° - 10°) due to the use of statistical data on the meteorological parameters of the region. However, the existing empirical models do not have the ability to take into account the peculiarities of the real behavior of the troposphere, which is manifested at low viewing angles, the work on which makes it possible to estimate the refractive characteristics of the propagation path. A comparison of the proposed mapping function with the most common models is shown in fig. 4.
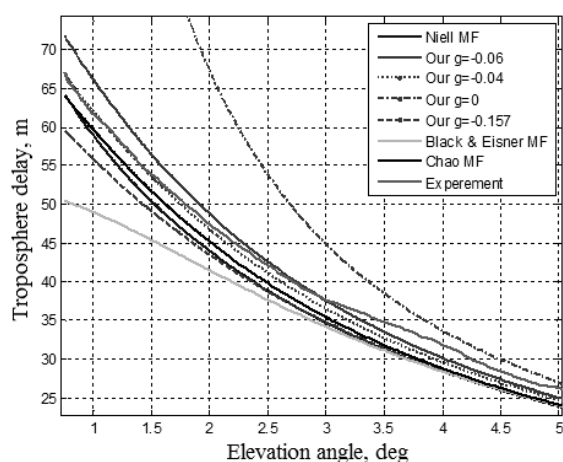

Fig. 4. Comparison of the proposed mapping function (MF) for various gradients of the refractive index with the most common models

As can be seen from Fig. 4, using the value

of the refractive index gradient in the model of the equivalent radius of the Earth allows taking into account the increase in the level of delay with increasing refraction. Thus, the proposed mapping function allows minimizing discrepancies between the model and the experimental data on tropospheric delay, to determine the gradient of the refractive index on the signal propagation path. To test the efficiency of the proposed method, satellite runs were analyzed in different seasons of the year and optimal values of the refractive index gradient were selected, at which the model maximally approached the experimental data (table 1).

In addition to obtaining information on the characteristics of the troposphere and the ionosphere using global navigation systems, it is possible to obtain information about characteristics of the underlying surface, which has recently attracted interest from researchers [11]. The physical prerequisite for such diagnostics can be the fact that when a navigation message is transmitted from a satellite, both the direct and surface reflected signals are recorded on the receiving side, bearing information about its properties and characteristics. Analyzing the behavior of the signal-to-noise ratio at the observation point at low elevation angles of the satellite and for various azimuth directions, it is possible to detect reflecting regions on the Earth's surface and also to estimate the type of surface and the degree of its roughness in a given direction [12].

Table 1. Estimate of g_N by meteorological parameters and the proposed model

Date	Refraction index, N-un.	g_N estimated by meteorological parameters, N-un./m	g_N estimated by proposed model, N-un./m
2012/07/06	321	− 0.0458	− 0.0466
2012/06/06	340	− 0.051	− 0.0504
2014/01/30	311.5	− 0.0391	− 0.0392
2014/03/08	305	− 0.0361	− 0.0356

It is shown that in the presence of reflection regions on the underlying surface in the received signal-to-noise ratios from individual satellites, which fly in similar azimuth directions, characteristic fluctuations appear, which are formed due to the interference of the direct and reflected signal (fig. 5). The signal at the reception point in the presence of multipath

in the propagation channel can be written as the sum of the harmonic components. Due to the change in the angle of sight of the source that is observed in vertical sections of the field above the media interface, due to the movement of the artificial satellite of the global navigation system and the height of the arrangement of the reflecting layers, components in the fluctuation spectrum of the attenuation factor appear, the frequency of which is related to the angular position of the source. This means that the angular position of the source can be determined from the frequency of the component using spectral analysis and the reflection coefficient by its intensity.
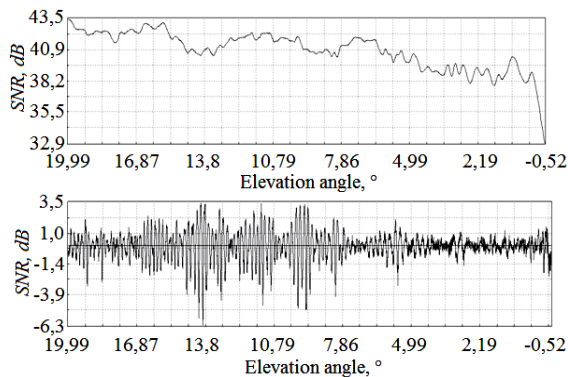

Fig. 5. Trend and fluctuation of SNR components of the received GPS-satellite signal

To analyze the type of the underlying surface, the dispersion level of the fluctuation component can be used. For example, the presence of building zones can lead to an increase in the dispersion level by a factor of 3 in comparison with the plain terrain (fig. 6).
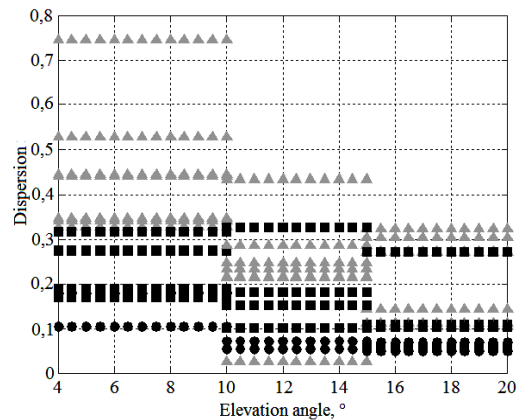

Fig. 6. Levels of variance for different types of terrain (●- fields, ■- buildings at the antenna level, ▲- buildings below the level of the antenna), depending on the elevation angle

The presence of characteristic sites under various refractive conditions (the dynamics and amplitude in the refractive index change in summer are much larger than in winter) is stable for all satellites, which indicates the stability of the effect. Thus, if the changes in the fluctuation component are quite clearly repeated for different satellites, it indicates presence of reflection regions which leads to such changes in the signal. The estimation of the parameters and location of the reflection region is performed by spectral analysis of the received signal level and the known trajectory of the analyzed satellites (fig. 7).
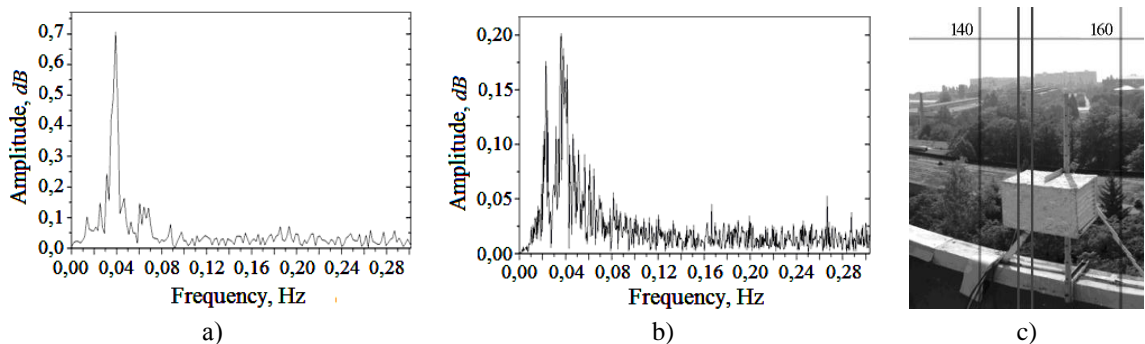

Fig. 7. Analysis of the reflection regions: a) the spectrum of the section corresponding to the anticipated reflection region, b) the spectrum of the complete satellite flight, c) the panorama of the terrain (the selected area corresponds to the direction to the reflection region)

Thus, the analysis of reflected signals from the Earth's surface can be used to analyze the characteristics of the underlying surface under various conditions (in the presence of snow cover, vegetation, etc.) and also for the detection of regions of reflection, the known position of which can be used to form the zeros of the antenna patterns of the receivers, thereby reducing errors in estimating the coordinates associated with multipath.

CONCLUSION

The use of data from single-frequency GNSS receivers for the diagnosis of the troposphere and the underlying surface is proposed. It is shown that the analysis of changes in the increments of pseudoranges and coordinate information in normal geomagnetic conditions can give information about the areas of rain passage and the space-time changes in the refractive index of the troposphere around the point of navigation measurements. A mapping function that makes it possible to determine the gradient of the refractive index on the propagation path of satellite signals on the basis of minimizing discrepancies between model and experimental data is proposed.

REFERENCES

1. Solheim, F. S., Vivekanandan, J., Ware, R. H., and Rocken, C., 1999. Propagation delays induced in GPS signals by dry air, water vapor, hydrometeors, and other particulates. *Journal of Geophysical Research: Atmospheres*, **104**(D8), 9663-9670.

2. Bevis, M., Businger, S., Herring, T. A., Rocken, C., Anthes, R. A., and Ware, R. H., 1992. GPS meteorology: Remote sensing of atmospheric water vapor using the Global Positioning System. *Journal of Geophysical Research: Atmospheres*, **97**(D14), 15787-15801.

3. Eminov, R. A., 2012. Some questions on calculation of tropospheric delay of the signal in navigation systems GLONASS/GPS, *T-Comm,* (4)*,* 40-41.

4. Schüler, T., 2001. On ground-based GPS tropospheric delay estimation. *Univ. der Bundeswehr München*.

5. Emardson, T. R., and Derks, H. J., 2000. On the relation between the wet delay and the integrated precipitable water vapour in the European atmosphere. *Meteorological Applications*, **7**(1), 61-68.

6. Nikol'Skii, V. V., and Nikol'Skaia, T. I. I., 1989. Electrodynamics and propagation of radio waves. *Moscow Izdatel Nauka*.

7. Krasyuk N.P., Koblov V. L., Krasyuk V. N., 1988. Influence of the troposphere and the underlying surface on the operation of the radar station, Moscow: Radio and Communication, Pp. 213.

8. Kravchenko, V. F., Kravchenko, O. V., Lutsenko, V. I., Lutsenko, I. V., and Popov, D. O., 2015. Usage of global navigation systems for detection of dangerous meteorological phenomena. *Journal of Measurement Science & Instrumentation*, **6**(1), 68-74.

9. Kovorotny A. L., Gorobets V. N., Goncharenko Yu. V., Rymar S. I., 2012., Measuring complex of the decimeter range for diagnostics of propagation conditions of radio waves in the atmosphere. *Bulletin of the National Technical University "KhPI": New solutions in modern technologies. - Kharkov: NTU "KhPI",* No. 17, pp. 11-16.

10. Lutsenko, V. I., Lutsenko, I. V., Popov, D. O., Laush, A. G., and Gudkov, V. N., 2014. Simulation of the mapping function for calculation of troposheric zenith delay. *Telecommunications and Radio Engineering*, **73**(5), 413-424.

11. Jin, S., and Komjathy, A., 2010. GNSS reflectometry and remote sensing: New objectives and results. *Advances in Space Research*, **46**(2), 111-117.

12. Lutsenko V. I., Popov D. O., Lutsenko I. V., 2016. Investigation of the underlying surface using radiation of the global navigation satellite system, *Radiophysics and Electronics,* Pp. 31-39.